

Potentially Predictive Variance Reducing Subsample Locations in Local Gaussian Process Regression

Chih-Li Sung^a, Robert B. Gramacy^b, Benjamin Haaland^a

^aGeorgia Institute of Technology

^bUniversity of Chicago

December 9, 2024

Abstract

Gaussian process models are commonly used as emulators for computer experiments. However, developing a Gaussian process emulator can be computationally prohibitive when the number of experimental samples is even moderately large. Local Gaussian process approximation (Gramacy and Apley, 2015) has been proposed as an accurate and computationally feasible emulation technique. Constructing sub-designs specific to predictions at a particular location of interest remains a substantial computational bottleneck. In this paper, two computationally efficient neighborhood search limiting techniques are proposed, a maximum distance method and a feature approximation method. Two examples demonstrate that the proposed methods indeed save substantial computation while retaining emulation accuracy.

1 Introduction

Due to continual advances in computational capabilities, researchers across fields increasingly rely on computer simulations in lieu of prohibitively costly or infeasible physical experiments. One example is Eckstein (2013), who investigate computer simulations of the interaction of energetic particles with solids. Physical effects such as elastic energy loss when a particle penetrates a solid, particle transmission through solids, and radiation damage are explored. These processes can be approximated by simulating the trajectories of all moving particles in a solid based on mathematical models. An example in linguistics is the study of language evolution (Cangelosi and Parisi, 2012), which is made challenging by the unobservable nature of language origin. Modeling techniques such as genetic algorithms can be used to simulate the process of natural selection and make it possible to explore a virtual evolution. While computer simulations provide a feasible alternative to many physical experiments, simulating from mathematical models is often itself expensive, in terms of both time and computation, and many researchers seek inexpensive approximations to their computationally demanding computer models.

Gaussian process (GP) models (Sacks et al., 1989) play an important role as emulators for computationally expensive computer experiments since they provide an approximation to the relationship between simulation output and untried inputs at a reduced computational cost. A major challenge in building a GP emulator for a large-scale computer experiment is that such an emulator requires inversion of a large ($N \times N$) correlation matrix. For dense matrices, this inversion step requires around $O(N^3)$ time, where N is the number of experimental runs. Inference for unknown parameters can demand hundreds of such inverses to evaluate the likelihood, and its derivatives, under different parameter settings for even the simplest Newton-based maximization schemes. This means that for a computer experiment with as few as $N = 10^4$ input-output pairs, accurate emulators cannot be constructed without specialized computing resources.

There are several recent approaches aimed at emulating large-scale computer experiments, most of which focus on approximation of the GP emulator. Examples include covariance tapering which replaces the dense correlation matrix with a sparse, tapered correlation matrix which is feasible to invert (Furrer et al., 2006), multi-step interpolation which successively models global, then more and more local behavior while controlling the number of non-zero entries in the correlation matrix at each stage (Haaland et al., 2011), and multiresolution modeling with Wendland’s compactly supported basis functions (Nychka et al., 2014). Alternatively, Paciorek et al. (2013) developed an R package called **bigGP** that combines symmetric-multiprocessors and GPU facilities to handle N as large as 67,275 without approximation. Nevertheless, computer model emulation is meant to avoid expensive computer simulation, not be a major consumer of it. Another approach, proposed by Plumlee (2014), is to sample input-output pairs according to a specific design structure, which leads to substantial saving in building an GP emulator. The method, however, is somewhat limited in practice due to its restriction to sparse grid designs.

In this paper, a local GP approach (Gramacy and Apley, 2015) is considered. The approach is modern, scalable and easy to implement with limited resources. The essential idea focuses on approximating the GP emulator at a particular location of interest via a relatively small subset of the original design, thus requiring only a modest subset of the rows and columns of the large ($N \times N$) covariance matrix for inversion. This process is then repeated across locations of interest, ideally largely in parallel. The determination of this local subset for each location of interest is crucial since it greatly impacts the accuracy of the corresponding local GP emulator. Gramacy and Apley (2015) proposed a greedy search to sequentially augment the subset according to an appropriate criteria and that approach yields reasonably accurate GP emulators. More details are presented in Section 2.

A bottleneck in this approach, however, is that the iterative search for the augmenting point requires looping over $O(N)$ data points at each iteration. In Section 3, motivated by the intuition that there is little potential benefit in including a data point far from the prediction location, two new neighborhood search limiting techniques are proposed, the *maximum distance method* and the *feature approximation method*. Two examples in Section 4 show that the proposed methods substantially speed up the local GP approach while retaining its accuracy. A brief discussion follows in Section 5. Mathematical proofs are provided in the Appendix.

2 Preliminaries

A Gaussian process (GP) is a stochastic process whose finite dimensional distributions are defined via a mean function $\mu(x)$ and a covariance function $\Sigma(x, x')$, for p -dimensional inputs x and x' . In particular, for N input x -values, say X_N , which define the N -vector $\mu(X_N)$ and $N \times N$ matrix $\Sigma(X_N, X_N)$, and a corresponding N -vector of responses Y_N , Y_N has distribution $Y_N \sim \mathcal{N}(\mu(X_N), \Sigma(X_N, X_N))$. The process variance $\sigma^2 > 0$ is commonly separated from the process correlation function, $Y_N \sim \mathcal{N}(\mu(X_N), \sigma^2 \Phi(X_N, X_N))$, where the $N \times N$ matrix $\Phi(X_N, X_N) = (\Phi(x_i, x_j))$ is defined in terms of a correlation function $\Phi(\cdot, \cdot)$, with $\Phi(x, x) = 1$. As an example, consider the often-used separable *Gaussian correlation function*

$$\Phi_{\Theta}(x, x') = \exp \left\{ - \sum_{j=1}^d (x_j - x'_j)^2 / \theta_j \right\}, \quad \text{where } \Theta = (\theta_1, \dots, \theta_d), \theta_j > 0, j = 1, \dots, p. \quad (1)$$

Observe that correlation decays exponentially fast in the squared distance between x_j and x'_j at rate θ_j . With this choice, the sample paths are very smooth (infinitely differentiable) and the resulting predictor is an interpolator.

The GP model is popular because inference for $\mu(\cdot), \sigma^2$ and Θ is easy and prediction is highly accurate. A popular inferential choice is maximum likelihood, with corresponding log likelihood (up to an additive constant)

$$\ell(\mu, \sigma^2, \Theta) = - \frac{1}{2} \left\{ n \log(\sigma^2) + \log(\det(\Phi_{\Theta}(X_N, X_N))) + (Y_N - \mu(X_N))^T \Phi_{\Theta}^{-1}(X_N, X_N) (Y_N - \mu(X_N)) / \sigma^2 \right\}$$

and the MLEs of $\mu(\cdot), \sigma^2$ and Θ are

$$(\hat{\mu}(\cdot), \hat{\sigma}^2, \hat{\Theta}) = \arg \max_{\mu, \sigma^2, \Theta} \ell(\mu, \sigma^2, \Theta). \quad (2)$$

Here, $\mu(\cdot)$ and its estimate are described somewhat vaguely. Common choices are $\mu(\cdot) \equiv 0$, $\mu(\cdot) = \mu$, or $\mu(\cdot) = h(\cdot)^T \beta$, for a vector of relatively simple basis functions $h(\cdot)$. More details on inference can be found in Fang et al. (2005) or Santner et al. (2013). Importantly, the predictive distribution of $Y(x)$ at a new setting x can be derived for fixed parameters by properties of the conditional multivariate normal distribution. In particular, it can be shown that $Y(x) | X_N, Y_N \sim \mathcal{N}(\mu_N(x), V_N(x))$, where

$$\mu_N(x) = \mu(x) + \Phi_{\Theta}(x, X_N) \Phi_{\Theta}^{-1}(X_N, X_N) (Y_N - \mu(X_N)), \quad (3)$$

$$V_N(x) = \sigma^2 (\Phi_{\Theta}(x, x) - \Phi_{\Theta}(x, X_N) \Phi_{\Theta}^{-1}(X_N, X_N) \Phi_{\Theta}(X_N, x)). \quad (4)$$

In a practical context, the parameters $\mu(\cdot), \sigma^2$, and Θ can be replaced by their estimates (2) and the corresponding predictive distribution is better approximated by a t -distribution than normal. Either way, $\hat{\mu}_N(x)$ is commonly taken as the *emulator*.

A major difficulty in computing the emulator (3) and its predictive variance (4) is solving the linear system $\Phi_{\Theta}(X_N, X_N) y = \Phi_{\Theta}(X_N, x)$, since it requires $O(N^2)$ storage and around

$O(N^3)$ computation for dense matrices. A promising approach is to search small sub-designs that approximate GP prediction and inference from the original design (Gramacy and Apley, 2015). The idea of the method is to focus on prediction at a particular generic location, x , using a subset of the full data $X_n(x) \subseteq X_N$. Intuitively, the sub-design $X_n(x)$ may be expected to be comprised of X_N close to x . With typical choices of $\Phi_\Theta(x, x')$, where correlation between elements x, x' in the input space decays quickly for x' far from x , x' 's which are far from x have vanishingly small influence on prediction. Ignoring them in order to work with much smaller, $n \times n$ matrices brings big computational savings, ideally with little impact on accuracy. Figure 1 displays a smaller sub-design ($n = 7$) near location $x = 0.5$ extracted from original design ($N = 21$). Although the emulator (red dashed line) performs very poorly from 0 to 0.3 and from 0.6 to 1.0, the sub-design provides accurate and robust prediction at $x = 0.5$.

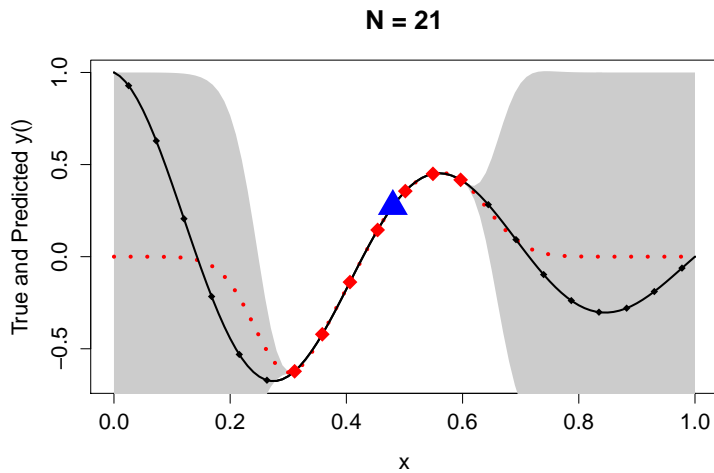


Figure 1: An example sub-design $X_7(x)$ for a one dimensional input. Black dots represent the full design, X_{21} , the blue triangle represents the point of interest $x = 0.5$ and the red diamonds represent the sub-design, $X_7(x)$. Based on the sub-design $X_7(x)$, the emulator is represented as the red dotted line, with the gray shaded region providing a pointwise 95% confidence band.

For an accurate and robust emulator, a smaller predictive variance (4) for each x is desirable. We seek a small sub-design $X_n(x) \subseteq X_N$ for each location of interest x , which minimizes the predictive variance (4) corresponding to the sub-design $X_n(x)$. This procedure is then repeated for each location of interest x . The identification of sub-designs and subsequent prediction at each such x can be parallelized immediately, providing a huge leap in computational scalability. However, searching for the optimal sub-design, which involves choosing n from N input sites, is a combinatorially huge undertaking. A sensible idea is to build up $X_n(x)$ by n nearest neighbors (NNs) close to x and the result is a valid probability model for $Y(x)|X_n(x), Y(X_n(x))$ (Datta et al., 2015). Gramacy and Apley (2015) proposed a greedy, iterative search for the sub-design, starting from a small NN set X_{n_0} and sequentially choosing x_{j+1} which provide the greatest reduction in predictive variance to augment $X_j(x)$,

for $j = n_0, n_0 + 1, \dots, n$. That is,

$$x_{j+1} = \arg \min_{u \in X_N \setminus X_j(x)} V_j(u). \quad (5)$$

Both the greedy and NN schemes can be shown to have computational order $O(n^3)$ when the scheme is efficiently deployed for each update $j \rightarrow j + 1$.

However, searching for the next design point in $X_N \setminus X_j(x)$ minimizing the predictive variance (5) is still computationally expensive, especially when the design size N is very large. For example, the new x_{j+1} based on (5) involves searching over $N - j$ candidates. In that case, the greedy search method still contains a serious computational bottleneck in spite of its improvements relative to solving the linear system in (3) for GP prediction and inference. Gramacy et al. (2014) recognized this issue and accelerated the search by exporting computation to graphical processing units (GPUs). They showed that the GPU scheme with local GP approximation and massive parallelization can lead to an accurate GP emulator for a one million run full design, with the GPUs providing approximately an order of magnitude speed increase. Gramacy and Haaland (2015) noticed that the progression of $x_{j+1}, j = 1, 2, \dots$ behaves *qualitatively* like ribbons and rings and suggested a computationally efficient heuristic based on one dimensional searches along rays emanating from the predictive location of interest x .

In Section 3, two computationally efficient and accuracy preserving neighborhood search methods are proposed. Both neighborhood searches reduce computation by decreasing the number of candidate design points examined. It is shown that only locations within a particular distance of either the prediction location x or the current sub-design, or locations in particular regions within a *feature space*, can have *substantial* influence on prediction. Using these techniques, it is possible to search a *much* smaller candidate set at each stage, leading to huge reductions in computation and increases in scalability.

3 Reduced Search in Local Gaussian Process

As discussed previously, when building a sub-design $X_n(x)$ for prediction at location x , there is intuitively little potential benefit to considering input locations which are very distant from x (relative to the correlation decay) as the response value at these locations is nearly independent of the response at x . In Section 3.1, a *maximum distance* bound and corresponding algorithm are provided and in Section 3.2, a *feature approximation* bound and corresponding algorithm are provided. The algorithms, in particular when used in concert, furnish a dramatically reduced set of potential design locations which need to be examined, in a computationally efficient and scalable manner.

3.1 Maximum Distance Method

Following the notation from Section 2, x is the particular location of interest, in terms of emulation/prediction, and $X_j(x)$ is the greedy sub-design at stage j . To build the sub-design $X_j(x)$, the locations which are distant from x intuitively should have little potential to reduce

the predictive variance at x . Therefore their consideration as potential x_{j+1} values, yielding $X_{j+1}(x)$, brings little benefit. This intuition is correct and developed as follows.

First, assume that the underlying correlation function is radially decreasing after appropriate linear transformation of the inputs. That is, assume there is a strictly decreasing function ϕ so that $\Phi_{\Theta}(x, x') = \phi(\|\Theta(x - x')\|_2)$ for some Θ . In the case of Θ arising from a separable Gaussian correlation structure, it has been shown that the lengthscale θ_j -values can be consistently estimated from data subsets in a computationally tractable way, even with large N (Liu and Hung, 2015). Now, consider a candidate input location x_{j+1} at stage $j + 1$ of the greedy sub-design search for an input location to add to the design and define $d_{\min}(x_{j+1})$ as the minimum (Mahalanobis-like) distance between the candidate point x_{j+1} and the current design and location of interest, that is,

$$d_{\min}(x_{j+1}) = \min\{\|\Theta(x - x_{j+1})\|_2, \|\Theta(x_i - x_{j+1})\|_2 : x_i \in X_j(x)\}. \quad (6)$$

For example, consider the sub-design $X_j(x)$ with two dimensional inputs shown in Figure 2 for $j = 6$. The location of interest is marked with a circled \times and the current sub-design $X_j(x)$ is indicated with gray dots. The candidate points x_{j+1} with $d_{\min}(x_{j+1})$ less than 0.8 lie within the yellow shaded region.

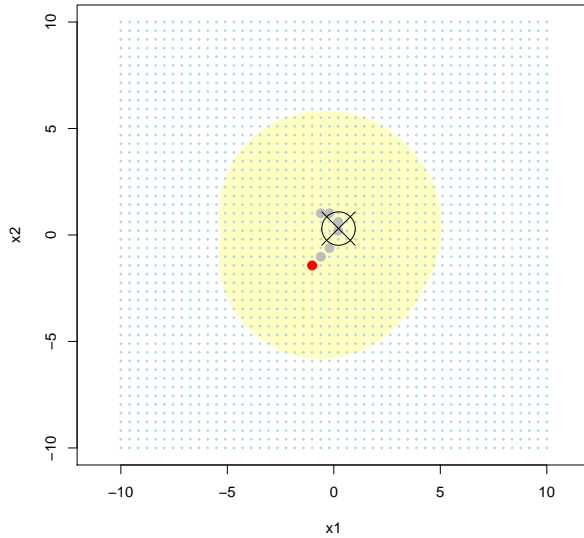


Figure 2: An example sub-design $X_6(x)$ with two dimensional inputs. The circled \times represents the location of interest. The gray dots represent current design points $X_6(x)$, the red dot represent the new input location x_7 , and the yellow shaded region represents the candidate points x_7 with $d_{\min}(x_7) < 0.8$.

Based on the local design scheme introduced in Section 2 and equation (5), the sub-design $X_n(x)$ is built up through the choices of x_{j+1} to sequentially argument $X_j(x)$, at each stage aiming to minimize predictive variance. Proposition 1 provides an alternate formula for this variance, which will be used to greatly reduce the number of candidates in the minimization problem. Its proof is provided in Appendix 6.1.

Proposition 1. *The predictive variance $V_j(x)$ in (4) can be represented via the recurrence*

$$V_{j+1}(x) = V_j(x) - \sigma^2 R(x_{j+1}).$$

Here, $R(x_{j+1})$ represents the (scaled) reduction in variance. In particular,

$$R(x_{j+1}) = \frac{(\Phi_{\Theta}(x, x_{j+1}) - \Phi_{\Theta}(x_{j+1}, X_j)\Phi_{\Theta}^{-1}(X_j, X_j)\Phi_{\Theta}(X_j, x))^2}{\Phi_{\Theta}(x_{j+1}, x_{j+1}) - \Phi_{\Theta}(x_{j+1}, X_j)\Phi_{\Theta}^{-1}(X_j, X_j)\Phi_{\Theta}(X_j, x_{j+1})}. \quad (7)$$

This recurrence relation is useful for searching candidates to entertain. Further, minimizing variance after adding the new input location x_{j+1} is equivalent to maximizing reduction in variance $R(x_{j+1})$.

The following theorem allows one to narrow the window of candidate locations to consider when searching greedily for a local design. The proof is provided in Appendix 6.2.

Theorem 1. *Suppose $\Phi : \Omega \times \Omega \rightarrow \mathbb{R}$ is a symmetric positive-definite kernel on a compact set $\Omega \subseteq \mathbb{R}^d$ and there exists a strictly decreasing function $\phi : \mathbb{R}^+ \rightarrow \mathbb{R}$ such that $\Phi_{\Theta}(x, y) = \phi(\|\Theta(x - y)\|_2)$ for some Θ . Then, for $\delta > 0$, $R(x_{j+1}) \leq \delta$ if*

$$d_{\min}(x_{j+1}) \geq \phi^{-1} \left(\sqrt{\frac{\delta}{(1 + \sqrt{j}\|\Phi_{\Theta}^{-1}(X_j, X_j)\Phi_{\Theta}(X_j, x)\|_2)^2 + j\delta/\lambda_{\min}}} \right), \quad (8)$$

where λ_{\min} is the minimum eigenvalue of $\Phi_{\Theta}(X_j, X_j)$.

This result indicates that candidate locations which are sufficiently distant from both the location of interest and the current sub-design do not have potential to reduce the variance more than δ . Importantly, if the full set of design locations X_N is stored in a data structure such as a *k-d tree* (Bentley, 1975), then the set of candidate locations which do not satisfy inequality (8) can be identified in $O(\log N)$ time, with constant depending on δ , dimension of the input space, and stage j , which provides a computationally efficient and readily scalable technique for reducing the set of potential candidate locations.

Theorem 1 suggests Algorithm 1 as a starting point for efficiently selecting sub-designs for prediction at location x . In the algorithm, a larger value of δ is desirable since larger δ leads to fewer candidate design locations to search. One way to obtain a relatively large value of δ is to examine the variance reductions on the set of k nearest neighbors which are not yet in the sub-design, which is shown in Step 2. The number of nearest neighbors k is a tuning parameter. A larger value of k will provide a larger variance reduction and therefore exclude more candidate design locations, albeit at an additional computational expense since the variance reduction must be checked at each of these locations. Alternatively, a large value of δ could be obtained by applying the heuristic proposed in Gramacy and Haaland (2015). From the result of Theorem 1, $T(X_j)$ in Step 3, which indicates the region such that

$$d_{\min}(x_{j+1}) \leq \phi^{-1} \left(\sqrt{\frac{\delta}{(1 + \sqrt{j}\|\Phi_{\Theta}^{-1}(X_j, X_j)\Phi_{\Theta}(X_j, x)\|_2)^2 + j\delta/\lambda_{\min}}} \right),$$

gives the subset of candidate locations that have potential to reduce the variance more than

δ . For each update $j \rightarrow j + 1$, the algorithm involves computation $O(j^3 + j \log N)$ in Step 3, $O(j^3)$ for computing y and $O(j \log N)$ searching.

Algorithm 1 maximum distance search method in local Gaussian process.

- 1: Set $j = 1$ and x_1 as the point closest to the predictive location x . Throughout, let $X_j(x) \equiv X_j = \{x_1, x_2, \dots, x_j\}$, dropping the explicit (x) argument.
- 2: Let $N_{jk}(x_j)$ denote the k nearest neighbors to x_j in $X_N \setminus X_j$, the candidate locations not currently in the sub-design. Set δ_{j+1} equal to the maximum variance reduction from $N_{jk}(x_j)$. That is,

$$\delta_{j+1} = \arg \max_{u \in N_{jk}(x_j)} R(u), \quad (9)$$

where $R(\cdot)$ is shown in (7).

- 3: Set $y = \phi^{-1} \left(\sqrt{\frac{\delta_{j+1}}{(1 + \sqrt{j} \|\Phi_{\Theta}^{-1}(X_j, X_j) \Phi_{\Theta}(X_j, x)\|_2)^2 + j \delta_{j+1} / \lambda_{\min}}} \right)$, where $\Phi_{\Theta}(x, x') = \phi(\|\Theta(x - x')\|_2)$ and λ_{\min} is the minimum eigenvalue of $\Phi_{\Theta}(X_j, X_j)$. Let

$$T(X_j) = \{u \in X_N \setminus X_j : \|\Theta(u - v)\|_2 \leq y \text{ for some } v \in \{x, X_j\}\}. \quad (10)$$

Then,

$$x_{j+1} = \arg \max_{u \in T(X_j)} R(u).$$

- 4: Set $j = j + 1$ and repeat 2 and 3 until the reduction in variance $R(x_{j+1})$ falls below a prespecified threshold or the local design budget is met.
-

3.2 Feature Approximation Method

In addition to the maximum distance method and associated algorithm, an approximation via eigen-decomposition can be applied to reduce the potential locations in a computationally efficient manner. Suppose that Φ is a symmetric positive-definite kernel on a compact set $\Omega \subseteq \mathbb{R}^d$ and $P : L_2(\Omega) \rightarrow L_2(\Omega)$ is a integral operator, defined by

$$Pv(x) := \int_{\Omega} \Phi(x, y)v(y)dy, \quad v \in L_2(\Omega), \quad x \in \Omega. \quad (11)$$

Then, Mercer's theorem guarantees the existence of a countable set of positive eigenvalues $\{\lambda_j\}_{j=1}^{\infty}$ and a orthonormal set $\{\varphi_j\}_{j=1}^{\infty}$ in $L_2(\Omega)$ consisting of the corresponding eigenfunctions of P , that is, $P\varphi_j = \lambda_j\varphi_j$ (Wendland, 2004). Furthermore, the eigenfunctions φ 's are continuous on Ω and Φ has the absolutely and uniformly convergent representation

$$\Phi(x, y) = \sum_{j=1}^{\infty} \lambda_j \varphi_j(x) \varphi_j(y).$$

In particular, Φ can be approximated uniformly over inputs in terms of a finite set of

eigenfunctions

$$\Phi(x, y) \approx \sum_{j=1}^D \lambda_j \phi_j(x) \phi_j(y) \quad (12)$$

for some moderately large integer D . For some kernel functions, closed form expressions exist. For example, the Gaussian correlation function (1) has eigenfunctions given by products of Gaussian correlations and Hermite polynomials (Zhu et al., 1997). More generally, Williams and Seeger (2001) show high-quality approximations to these eigen-decompositions can be obtained via Nyström’s method.

Theorem 2. *Assume $\Phi : \Omega \times \Omega \rightarrow \mathbb{R}$ is a symmetric positive-definite kernel on compact set $\Omega \subseteq \mathbb{R}^d$ which can be approximated via D eigenfunctions (see equation (12)). Then, the reduction in variance (7) has approximate representation*

$$R(x_{j+1}) \approx \|C_{X_j}(x)\|_2^2 \cos^2(\vartheta), \quad (13)$$

where ϑ is the angle between $C_{X_j}(x)$ and $C_{X_j}(x_{j+1})$,

$$\begin{aligned} C_{X_j}(t) &= [I - U(X_j)[U^T(X_j)U(X_j)]^{-1}U^T(X_j)]U(t), \\ U(t) &= \left(\sqrt{\lambda_1}\varphi_1(t), \dots, \sqrt{\lambda_D}\varphi_D(t)\right)^T, \quad \text{and} \\ U(X_j) &= [U(x_1), \dots, U(x_j)], \end{aligned} \quad (14)$$

for eigenfunctions $\varphi_i(t)$ and corresponding ordered eigenvalues $\lambda_1 \geq \dots \geq \lambda_D$.

Proof. Provided in Appendix 6.3. □

According to this approximation, instead of excluding candidates in Euclidean space as indicated in Theorem 1, the reduced set can be further reduced by transforming the reduced set of inputs into feature space. A modified algorithm is suggested as follows. The variance reduction threshold in equation (9) now places a restriction on the *angle* between $C_{X_j}(x)$ and $C_{X_j}(x_{j+1})$, where we would like to exclude points *outside* the cones

$$\cos^2(\vartheta) \leq \frac{\delta_{j+1}}{\|C_{X_j}(x)\|_2^2}. \quad (15)$$

A feature approximation modification to Algorithm 1 is shown in Algorithm 2. To reduce the computational burden in checking (15), the values of the first D eigenfunctions at the full dataset $X_N, U(X_N)$, could be computed in advance and stored based on locality-sensitive hashing (LSH) scheme (Indyk and Motwani, 1998). LSH is a method for answering approximate similarity-search queries in high-dimensional spaces. The basic idea is to use special locality-sensitive functions to *hash* points into “buckets” such that “nearby” points map to the same bucket with high probability. Many similarity measures have corresponding LSH functions that achieve this property. For instance, the hashing functions for cosine-similarity are the normal vectors of random hyperplanes through origin, denoted for example as v_1, \dots, v_k . Depending on its side of these random hyperplanes, a point p is placed in

bucket $h_1(p), \dots, h_k(p)$, where $h_i(p) = \text{sign}(v_i^T p)$. Jain et al. (2008) showed for the pairwise similarity

$$\frac{y_k^T A_j y_h}{\sqrt{|G_j y_k| |G_j y_h|}},$$

where $y_k, y_h \in \mathbb{R}^d$, $G_j^T G_j = A_j$ and A_j is a $d \times d$ positive-definite matrix that is updated for each iteration j , the hash function can be defined as:

$$h_{A_j}(y) = \begin{cases} 1 & r^T G_j y \geq 0 \\ 0 & \text{otherwise} \end{cases}, \quad (16)$$

where the vector r is chosen at random from a d -dimensional Gaussian distribution. Let $G_j = I - U(X_j)[U^T(X_j)U(X_j)]^{-1}U^T(X_j)$ and $A_j = G_j^T G_j$, then $\cos(\vartheta)$ in (13) can be represented as

$$\cos(\vartheta) = \frac{U(x_{j+1})^T A_j U(x)}{\sqrt{|G_j U(x_{j+1})| |G_j U(x)|}}.$$

Thus, in the feature approximation method, LSH scheme can be employed by storing $U(X_N)$ in advance and updating the hash function (16) at each iteration, where y is replaced by $U(y)$. At query time, similar points are hashed to the same bucket with the query $U(x)$ and the results are guaranteed to have a similarity within a small error after repeating the procedure several times. In particular, for each update $j \rightarrow j+1$, given that the LSH method guarantees retrieval of points within the radius $(1 + \epsilon)M$ from the query point $U(x)$, where M is the distance of the true nearest neighbor from $U(x)$, the method requires $O(D^3 + DN^{1/(1+\epsilon)})$ computational time, $O(D^3)$ for updating matrix G_j , $O(D)$ for computing hash function $h_{A_j}(y)$ and $O(DN^{1/(1+\epsilon)})$ for identifying the hashed query (Jain et al., 2008), where D is the number of eigenfunctions in Theorem 2. In Section 4, two examples show the benefit from the LSH approach in the feature approximation method.

Algorithm 2 Feature approximation modification to Algorithm 1.

In Step 3 of Algorithm 1, replace $T(X_j)$ with $T^*(X_j)$, where

$$T^*(X_j) = \{u \in X_N \setminus X_j : \|\Theta(u - v)\|_2 \leq y \text{ and } \cos^2(\vartheta) \geq \delta_{j+1}/\|C_{X_j}(x)\|_2^2 \\ \text{for some } v \in \{x, X_j\}\},$$

and ϑ , $C_{X_j}(x)$ are defined in Theorem 2. Then,

$$x_{j+1} = \arg \max_{u \in T^*(X_j)} R(u).$$

As an illustration of how cones in feature space relate to the design space, consider a full design X_N consisting of 2500 Unif(0, 1) data points, shown in gray and yellow in the *left* panel of Figure 3. The correlation function is $\Phi(x, x') = \exp\{-\|(x - x')/10\|^2\}$ and the predictive location of interest is $x = (0.5, 0.5)$, shown as a black triangle in the *left* panel. The first 7 design points are chosen greedily and indicated with red numbers. The *right* panel shows the first 2 components of the feature space (the first two eigenfunctions evaluated at

the design points), colored and labeled correspondingly. The vector $C_{X_7}(x)$ is shown as the middle dotted line in the *right* panel, with $|\vartheta| \leq \pi/20$ shown as the outer dotted lines. Design points falling within these cones are shown in yellow in both panels. The design points in the *left* panel which fall in the yellow stripe have the most potential to reduce predictive variance.

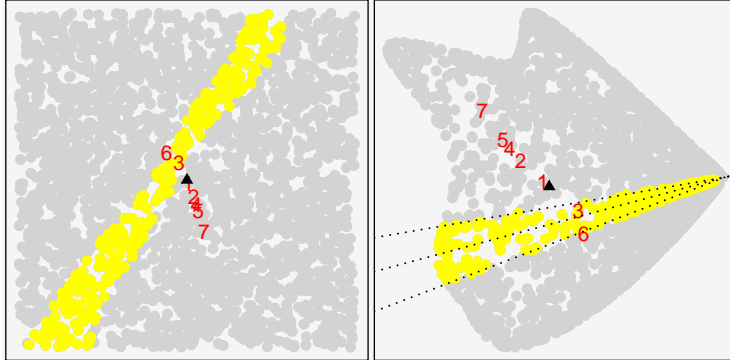


Figure 3: Gray and yellow dots represent design points in the original space (left) and a $D = 2$ dimensional feature space approximation (right). Location of interest and current design are annotated with black triangle and red numbers, respectively. Vector $C_{X_7}(x)$ and cones $|\vartheta| \leq \pi/20$ shown with dotted lines. Design points falling within these cones are shown in yellow in both panels.

The candidate set $T^*(X_j)$ might be expected to be much smaller than $T(X_j)$ if (i) the correlation function is well approximated by the finite set of eigenfunctions and eigenvalues and (ii) the dimension of input is not too large, since distance becomes a very powerful exclusion criteria in even moderately high-dimensional space. Section 4 presents two examples implementing the feature approximation algorithm and shows a smaller search space compared to the original maximum distance algorithm in Section 3.1.

4 Examples

Two examples are discussed in this section, a two-dimensional example which demonstrates the algorithm and visually illustrates the reduction of candidates, and a larger-scale, higher-dimensional example. Both examples show the proposed methods considerably outperforming the original search method with respect to computational time. All numerical studies were conducted using R (R Core Team, 2015) on a laptop with 2.4 GHz CPU and 8GB of RAM. The k-d tree and LSH were implemented via Python library SciPy (Jones et al., 2001) and modifications to the source code of the Python package scikit-learn (Pedregosa et al., 2011; Bawa et al., 2005), respectively. Both of them were conducted using R through the rPython package (Bellosta, 2015).

4.1 Two-dimensional problem of size $N = 50^2$

Consider a computer experiment with full set of design locations X_N consisting of a regular 50×50 grid on $[-10, 10]^2$ (2500 design points, light blue in Figure 4) and take the predictive location of interest x to be $(0.22, 0.30)$ (circled \times in Figure 4). Set $\sigma^2 = 1$ and consider the

Gaussian correlation function

$$\Phi_{\Theta}(x, y) = \exp \left\{ - \left(\frac{(x_1 - y_1)^2}{\theta_1} + \frac{(x_2 - y_2)^2}{\theta_2} \right) \right\},$$

with $\theta_1 = \theta_2 = 3$. This correlation function implies the ϕ in Algorithm 1 is $\phi(u) = \exp\{-u^2\}$ and $\Theta = (1/\theta_1, 1/\theta_2)$. Then, we have $\phi^{-1}(v) = \sqrt{-\log v}$.

Figure 4 illustrates the sub-design selection procedure shown in Algorithm 1, in which $k = 8$ nearest neighbors (from the candidate set) are used to generate the threshold in Step 2. In Figure 4, the gray dots represent the current design $X_j(x)$, the red dots represent the optimal augmenting point x_{j+1} , and the points which are excluded from the search for that location are those which fall outside the yellow shaded region. The panels in the figure correspond to greedy search steps $j \in \{3, 14, 27\}$. Notably, the optimal additional design points illustrated in Figure 4 are not always the nearest neighbors to the location of interest. In this example, only 7.44% (186/2500) of candidates need to be searched in the beginning. Even after choosing thirty data points, there is no need to search much more than half of the full data (53.40%=1335/2500).

Continuing the same example, Figure 4 also shows substantial improvement from the feature approximation method. In the example, a $D = 500$ dimensional feature space approximation (Williams and Seeger, 2001) is pre-computed. The points annotated with green +s are the points which are not excluded from the search. In fact, the number of candidates which need to be searched is usually reduced at least 10 fold and in many cases 50 or 100 fold, or more.

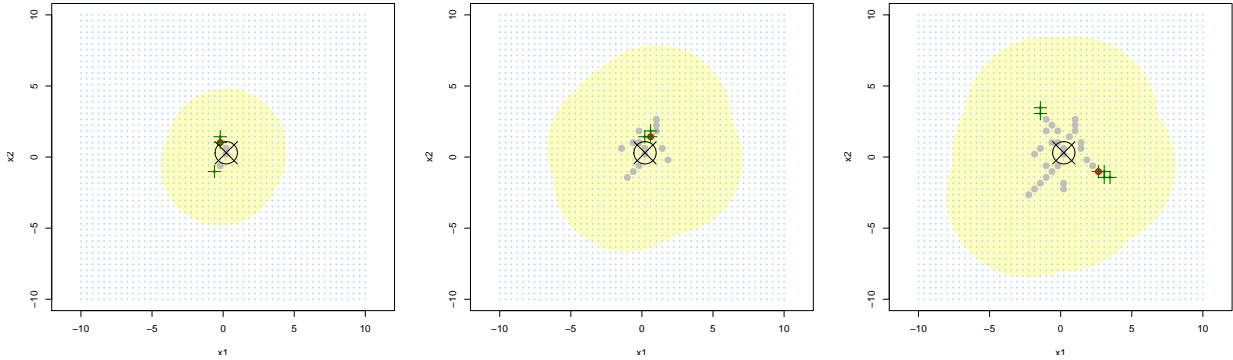


Figure 4: *Left, middle, and right panels respectively illustrate selection at $j = 3, 14,$ and 27 . The circled \times is the location of interest, $(0.22, 0.30)$. Gray dots are the current design points; red dots are the optimal x_{j+1} ; points which are excluded from the search based on the maximum distance method are those which fall outside the yellow shaded region. Points which are excluded from the search based on the feature approximation method are those which are not annotated with a green +.*

The approximation to the correlation function in the feature approximation method has the potential to result in a loss of variance reduction compared to the maximum distance method. Here the relative difference in variance

$$\frac{V_{j,FA}(x) - V_{j,MD}(x)}{V_{j,MD}(x)}$$

is used to measure the loss of variance reduction, where $V_{j,FA}(x)$ and $V_{j,MD}(x)$ are the variance of the emulator at predictive location x at stage j by using feature approximation method and maximum distance method, respectively. Table 1 shows the relative difference in variance resulting from the feature approximation method with $D = 10, 300$ and 500 features as compared to the maximum distance method. As expected, a larger number of features, $D = 500$, reduces the searched candidates without a loss in variance reduction. For $D = 300$, although there is a slight difference in variance, the discrepancy may be small enough to be ignored. At stage 10, 15 and 25, the variance is even smaller than the maximum distance method, due to the greedy nature of the maximum distance method. Notably, if a small number of features, say $D = 10$, is chosen, the feature approximation search offers little improvement over the maximum distance method in terms of search reduction even though the variance remains the same as the maximum distance method. In this case, $D = 300$ might be a reasonable choice of number of features balancing ease of computation and small predictive variance.

Relative Difference (# of searching candidates)	$D = 10$		$D = 300$		$D = 500$		Variance by Maximum Distance Method
Stage 10	0	(817)	-0.124	(1)	0	(51)	2.68×10^{-6} (817)
Stage 15	0	(939)	-0.101	(33)	0	(32)	9.53×10^{-7} (939)
Stage 20	0	(1179)	0.257	(26)	0	(197)	2.55×10^{-7} (1179)
Stage 25	0.002	(1122)	-0.103	(10)	0	(5)	1.30×10^{-7} (1184)
Stage 30	-0.742	(1265)	0.072	(3)	0	(5)	7.50×10^{-8} (1335)

Table 1: The relative difference in variance of the emulator at location $(0.22, 0.30)$ between the maximum distance search as a baseline and feature approximation search with number of features D : 10, 300 and 500. Baseline variance by maximum distance search is shown in the last column. The value in parentheses is the number of search candidates.

To compare with the exhaustive search, Table 2 shows the the computation time and proportion of searched candidates for the proposed methods and exhaustive search. The reduction in the number of searched candidates for the maximum distance method is from 100% to 54% and the method also speeds up the computational time from 482 to 195 seconds with a k-d tree data structure. On the other hand, although the feature approximation method needs 32 seconds for computing the features in advance, the number of searched candidates for feature approximation method with $D = 300$ is reduced to 0.53% at stage 30. The computational time, on a ordinary laptop, is less than 25 seconds for 30 stages of iteration in the $N = 50^2$ experiment. With a LSH approximate similarity-search method, it speeds up the search from 25 to 21 seconds while the proportions of candidates slightly differ from the real ones. It is worth noting that introducing the k-d tree and LSH data structure in this moderately-sized problem does not greatly improve on the computational cost (k-d tree: $236 \rightarrow 195$, LSH: $25 \rightarrow 21$). In a larger-scale problem, however, the improvements due to incorporating a k-d tree or LSH data structure can be significant, as will be shown in next subsection.

Seconds (Candidates %)	Exhaustive Search	Maximum Distance Method		*Feature Approximation Method with $D = 300$	
		w/o KD-tree	w/ KD-tree	w/o LSH	w/ LSH
Stage 10	73	20 (32.81%)	17 (32.81%)	5 (0.04%)	5 (0.20%)
Stage 15	141	45 (37.79%)	41 (37.79%)	9 (1.33%)	8 (0.04%)
Stage 20	232	90 (47.54%)	78 (47.54%)	14 (1.05%)	11 (0.65%)
Stage 25	344	149 (47.84%)	128 (47.84%)	19 (0.40%)	15 (0.04%)
Stage 30	482	236 (54.05%)	195 (54.05%)	25 (0.53%)	21 (0.12%)

Table 2: Time (seconds) comparison between exhaustive search and two proposed methods in two-dimensional setting with $N = 50^2$ at predictive location $x = (0.22, 0.30)$. The values in parantheses are the percentage searched of full design. *Pre-computation time for feature approximation method is 32 seconds.

4.2 30-dimensional problem of size $N = 10^4$

Even more substantial reductions in the number of search candidates are seen for both methods in a larger-scale, higher-dimensional setting. In this example, we generate a 30-dimensional Sobol sequence of size $N = 10^4$ in a $[-10, 10]^{30}$ design space and the predictive location is $x = (0.613, 0.613, \dots, 0.613)$. Set $\sigma^2 = 1$ and take correlation function $\Phi_{\Theta}(x, y) = \exp\{-\sum_{i=1}^{30} \frac{(x_i - y_i)^2}{\theta_i}\}$ with $\theta_i = 3, i = 1, \dots, 30$.

Table 3 shows the comparison between exhaustive search and the two proposed methods. As the table shows, the two proposed methods outperform exhaustive search in terms of computation time. Further, the number of candidates searched for both methods are less than 5% (= $500/10^4$) across all 30 stages. While the exhaustive search takes 20000 seconds (≈ 5.5 hours) for 30 stage iterations, less than 36 minutes are required for the maximum distance method. Incorporating a k-d tree data structure, the computational time decreases by more than three times (≈ 11 minutes). Compared with the previous example, incorporating a k-d tree data structure has substantial benefits in terms of computational time in this larger-scale setting.

The feature approximation method, as expected, has a smaller-sized candidate set than the maximum distance method and it is without any accuracy loss due to approximation. On the other hand, due to the moderately expensive computation in Algorithm 2 by using $D = 500$ features, in this example the feature approximation search is more time-consuming than the maximum distance method with a k-d tree. Of course, the computation of more features naturally incurs higher computational costs, but provides higher accuracy. In our example, computing the $D = 500$ features requires 374 seconds, but achieves high accuracy. With a LSH approximate similarity-search method, it reduces around 13 minutes computational time across all 30 stages. To sum up, the feature approximation approach outperforms exhaustive search and is efficient especially when the maximum distance approach is too conservative, such as the two-dimensional case in Section 4.1.

Seconds (Candidates %)	Exhaustive Search	Maximum Distance Method		*Feature Approximation Method with $D = 500$	
		w/o KD-tree	w/ KD-tree	w/o LSH	w/ LSH
Stage 10	2675	545 (0.42%)	56 (0.42%)	326 (0.41%)	198 (2.13%)
Stage 15	5424	847 (0.17%)	116 (0.17%)	593 (0.15%)	334 (1.62%)
Stage 20	9224	1206 (2.87%)	203 (2.87%)	887 (2.83%)	491 (2.49%)
Stage 25	14078	1626 (0.63%)	363 (0.63%)	1239 (0.60%)	763 (3.30%)
Stage 30	20000	2141 (4.73%)	654 (4.73%)	1720 (4.65%)	973 (0.79%)

Table 3: Time (seconds) comparison between exhaustive search and two proposed methods in 30-dimensional setting with $N = 10^4$ at predictive location $x = (0.613, 0.613, \dots, 0.613)$. The values in bracket shows the percentage searched of full design. *Pre-computation time for feature approximation method is 374 seconds.

5 Conclusion and Discussion

Emulators have become crucial for approximating the relationship between input and output in computer simulations. However, as the data sizes continue to grow, GP emulators fail to perform well due to memory, computation, and numerical issues. In order to deal with these issues, Gramacy and Apley (2015) proposed a local GP emulation technique accompanied by a sequential scheme for building local sub-designs by maximizing reduction in variance. We showed that an important (exhaustive) search subroutine could be substantially shortcut without compromising on accuracy, leading to substantial reductions in computing time.

In particular, using the distance-based structure of most correlation functions in GP models, we showed that input locations distant from the predictive location offer little potential variance reduction. We proposed a *maximum distance method* to speed up construction of local GP emulators on the neighborhood of the existing sub-design and predictive location. Taking a step further, we observed that, since the correlation functions in GP models can be uniformly approximated by a finite sum of features via eigen-decomposition, mapping original space into feature space by the eigenfunctions can further reduce the search space. We developed a *feature approximation method* that determines viable candidates in terms of the angle between two projected feature vectors. This leads to an even smaller proportion of viable candidates for searching. Taken together, the two reductions lead to an orders of magnitude smaller search set.

We provided two examples that illustrate how the two search methods perform. It takes only take few minutes, on an ordinary laptop, to obtain accurate predictions in large-scale problems. In particular, the maximum distance search leveraging a k-d tree data structure takes less than 11 minutes to search effective candidates. A full search, by comparison, takes more than five hours.

An implicit disadvantage of these methods is the impact of the correlation parameters. Take the example in Figure 2, where $d_{\min}(x_6) < 0.8$. From the definition (6) of $d_{\min}(x_{j+1})$, suppose $\Theta = (1/\theta, 1/\theta)$, then the larger θ is, the bigger the search area, the yellow shaded region in Figure 2. The reason is that when θ is large, the correlation is close to one and the

data points tend to be highly correlated, implying that every data point in the full design carries important information for each predictive location. In other words, the algorithm requires more computation for the “easier” problem—i.e., with a “flatter” surface. On the other hand “flatter” surfaces will not require large sub-designs to achieve small predictive variance.

An improvement worth exploring is how to determine of the number of features D in the feature approximation method. Cross-validation to minimize variance of a emulator may present an attractive option. Finally, a discussion of the choice between maximum distance method and feature approximation method might be desirable. Although the maximum distance method was being combined with the feature approximation method and that guarantees a smaller candidate set in the feature approximation method, pre-computation of the features constitutes a moderately expensive sunk computational cost. In the example in Section 4.2, 374 seconds were required to pre-compute 500 features. In either case, the two methods outperform exhaustive search as shown in Table 3.

6 Appendices

6.1 Proof of Proposition 1

In the variance definition (4), the variance of $Y(x)$ at stage $j + 1$ is

$$V_{j+1}(x) = \sigma^2 \{ \Phi_{\Theta}(x, x) - \Phi_{\Theta}(x, X_{j+1}) \Phi_{\Theta}^{-1}(X_{j+1}, X_{j+1}) \Phi(X_{j+1}, x) \}. \quad (17)$$

Since X_{j+1} is comprised of X_j and x_{j+1} , (17) can be rewritten as

$$V_{j+1}(x) = \sigma^2 \left\{ \Phi_{\Theta}(x, x) - \begin{bmatrix} \Phi_{\Theta}(x, x_{j+1}) & \Phi_{\Theta}(x, X_j) \end{bmatrix} \begin{bmatrix} \Phi_{\Theta}(x_{j+1}, x_{j+1}) & \Phi_{\Theta}(x_{j+1}, X_j) \\ \Phi_{\Theta}(X_j, x_{j+1}) & \Phi_{\Theta}(X_j, X_j) \end{bmatrix}^{-1} \begin{bmatrix} \Phi_{\Theta}(x, x_{j+1}) \\ \Phi_{\Theta}(X_j, x) \end{bmatrix} \right\}. \quad (18)$$

For simplicity, the second term of (18) can be written as a partitioned matrix, that is,

$$\begin{bmatrix} a_1^T & a_2^T \end{bmatrix} \begin{bmatrix} B_{11} & B_{12} \\ B_{21} & B_{22} \end{bmatrix}^{-1} \begin{bmatrix} a_1 \\ a_2 \end{bmatrix}, \quad (19)$$

where

$$a_1 = \Phi_{\Theta}(x, x_{j+1}), a_2 = \Phi_{\Theta}(X_j, x),$$

$$B_{11} = \Phi_{\Theta}(x_{j+1}, x_{j+1}), B_{12} = \Phi_{\Theta}(x_{j+1}, X_j) = B_{12}^T \text{ and } B_{22} = \Phi_{\Theta}(X_j, X_j).$$

Applying partitioned matrix inverse results (Harville, 1997) and simplifying (19) gives

$$a_2^T B_{22}^{-1} a_2 + (a_1 - B_{12} B_{22}^{-1} a_2)^T B_{11.2}^{-1} (a_1 - B_{12} B_{22}^{-1} a_2), \quad (20)$$

where $B_{11.2} = B_{11} - B_{12}B_{22}^{-1}B_{21}$.

Then, taking (20) into (18) leads to

$$\begin{aligned}
V(X_{j+1}) &= \sigma^2 \{ \Phi_{\Theta}(x, x) - a_2^T B_{22}^{-1} a_2 - (a_1 - B_{12}B_{22}^{-1}a_2)^T B_{11.2}^{-1} (a_1 - B_{12}B_{22}^{-1}a_2) \} \\
&= \sigma^2 \{ \Phi_{\Theta}(x, x) - \Phi_{\Theta}(x, X_j) \Phi_{\Theta}^{-1}(X_j, X_j) \Phi_{\Theta}(X_j, x) \\
&\quad - (a_1 - B_{12}B_{22}^{-1}a_2)^T B_{11.2}^{-1} (a_1 - B_{12}B_{22}^{-1}a_2) \} \\
&= V(X_j) - \sigma^2 \{ (a_1 - B_{12}B_{22}^{-1}a_2)^T B_{11.2}^{-1} (a_1 - B_{12}B_{22}^{-1}a_2) \} \\
&= V(X_j) - \sigma^2 R(x_{j+1}),
\end{aligned}$$

where

$$\begin{aligned}
R(x_{j+1}) &= (a_1 - B_{12}B_{22}^{-1}a_2)^T B_{11.2}^{-1} (a_1 - B_{12}B_{22}^{-1}a_2) \\
&= (a_1 - B_{12}B_{22}^{-1}a_2)^2 / B_{11.2} \\
&= \frac{(\Phi_{\Theta}(x, x_{j+1}) - \Phi_{\Theta}(x_{j+1}, X_j) \Phi_{\Theta}^{-1}(X_j, X_j) \Phi_{\Theta}(X_j, x))^2}{\Phi_{\Theta}(x_{j+1}, x_{j+1}) - \Phi_{\Theta}(x_{j+1}, X_j) \Phi_{\Theta}^{-1}(X_j, X_j) \Phi_{\Theta}(X_j, x_{j+1})},
\end{aligned}$$

and the second equality holds since $B_{11.2}$ is a scalar.

6.2 Proof of Theorem 1

Since $(a - b)^2 \leq (a + b)^2$ for $a, b \geq 0$, equation (8) can be bounded as

$$\begin{aligned}
R(x_{j+1}) &= \frac{(\Phi_{\Theta}(x, x_{j+1}) - \Phi_{\Theta}(x_{j+1}, X_j) \Phi_{\Theta}^{-1}(X_j, X_j) \Phi_{\Theta}(X_j, x))^2}{\Phi_{\Theta}(x_{j+1}, x_{j+1}) - \Phi_{\Theta}(x_{j+1}, X_j) \Phi_{\Theta}^{-1}(X_j, X_j) \Phi_{\Theta}(X_j, x_{j+1})} \\
&\leq \frac{(\Phi_{\Theta}(x, x_{j+1}) + \Phi_{\Theta}(x_{j+1}, X_j) \Phi_{\Theta}^{-1}(X_j, X_j) \Phi_{\Theta}(X_j, x))^2}{\Phi_{\Theta}(x_{j+1}, x_{j+1}) - \Phi_{\Theta}(x_{j+1}, X_j) \Phi_{\Theta}^{-1}(X_j, X_j) \Phi_{\Theta}(X_j, x_{j+1})}.
\end{aligned}$$

Also, since

$$a^T B^{-1} b \leq \|a\|_2 \|B^{-1} b\|_2$$

and

$$a^T B^{-1} a \leq \|a\|_2^2 \lambda_{\max}(B^{-1}) = \|a\|_2^2 / \lambda_{\min}(B),$$

where $\lambda_{\max}(\cdot)$ and $\lambda_{\min}(\cdot)$ denote the maximum and minimum eigenvalues of a specific matrix, respectively, the inequality becomes

$$R(x_{j+1}) \leq \frac{(\Phi_{\Theta}(x, x_{j+1}) + \|\Phi_{\Theta}(x_{j+1}, X_j)\|_2 \|\Phi_{\Theta}^{-1}(X_j, X_j) \Phi_{\Theta}(X_j, x)\|_2)^2}{1 - \|\Phi_{\Theta}(X_j, x_{j+1})\|_2^2 / \lambda_{\min}},$$

where λ_{\min} is the minimum eigenvalue of $\Phi_{\Theta}(X_j, X_j)$.

Furthermore, according to the definition $d_{\min}(x_{j+1})$ of the minimum (Mahalanobis-like) distance as (6) and the definition $\phi(\cdot)$ as in Theorem 1, we have

$$\Phi_{\Theta}(u, x_{j+1}) \leq \phi(d_{\min}(x_{j+1})), \text{ for any } u \in \{x, X_j\},$$

which also implies

$$\|\Phi_{\Theta}(x_{j+1}, X_j)\|_2 = \|\Phi_{\Theta}(X_j, x_{j+1})\|_2 \leq \sqrt{j}\phi(d_{\min}(x_{j+1})),$$

therefore the inequality can be bounded as

$$R(x_{j+1}) \leq \frac{(\phi(d_{\min}(x_{j+1})) + \sqrt{j}\phi(d_{\min}(x_{j+1})))\|\Phi_{\Theta}^{-1}(X_j, X_j)\Phi_{\Theta}(X_j, x)\|_2)^2}{1 - j\phi^2(d_{\min}(x_{j+1}))/\lambda_{\min}}. \quad (21)$$

Thus, for $\delta > 0$, if

$$\frac{(\phi(d_{\min}(x_{j+1})) + \sqrt{j}\phi(d_{\min}(x_{j+1})))\|\Phi_{\Theta}^{-1}(X_j, X_j)\Phi_{\Theta}(X_j, x)\|_2)^2}{1 - j\phi^2(d_{\min}(x_{j+1}))/\lambda_{\min}} \leq \delta$$

or equivalently

$$d_{\min}(x_{j+1}) \geq \phi^{-1}\left(\sqrt{\frac{\delta}{(1 + \sqrt{j}\|\Phi_{\Theta}^{-1}(X_j, X_j)\Phi_{\Theta}(X_j, x)\|_2)^2 + j\delta/\lambda_{\min}}}\right),$$

then by (21), $R(x_{j+1}) \leq \delta$.

6.3 Proof of Theorem 2

Define $U(t) = (\sqrt{\lambda_1}\phi_1(t), \sqrt{\lambda_2}\phi_2(t), \dots, \sqrt{\lambda_D}\phi_D(t))^T \in \mathbb{R}^{D \times 1}$, where $\phi_i(\cdot), i = 1, \dots, D$ is an orthonormal basis of $L^2(\Omega)$ consisting of the eigenfunctions of T , defined in (11), and $\lambda_1 \geq \lambda_2 \geq \dots \geq \lambda_D$ are corresponding eigenvalues. According to (12), the approximated eigen-decomposition can be rewritten as

$$\Phi(x, y) \approx U^T(x)U(y).$$

Also, define a matrix $U(K) = [U(k_1), U(k_2), \dots, U(k_n)] \in \mathbb{R}^{D \times n}$ for $K = (k_1, k_2, \dots, k_n)$. Then, the reduction in variance $R(x_{j+1})$ in (7) can be approximated to the following:

$$\begin{aligned} R(x_{j+1}) &= \frac{(\Phi_{\Theta}(x, x_{j+1}) - \Phi_{\Theta}(x_{j+1}, X_j)\Phi_{\Theta}^{-1}(X_j, X_j)\Phi_{\Theta}(X_j, x))^2}{\Phi_{\Theta}(x_{j+1}, x_{j+1}) - \Phi_{\Theta}(x_{j+1}, X_j)\Phi_{\Theta}^{-1}(X_j, X_j)\Phi_{\Theta}(X_j, x_{j+1})} \\ &\approx \frac{(U_{\Theta}^T(x_{j+1})U_{\Theta}(x) - U_{\Theta}^T(x_{j+1})U_{\Theta}(X_j)[U_{\Theta}^T(X_j)U_{\Theta}(X_j)]^{-}U_{\Theta}^T(X_j)U_{\Theta}(x))^2}{U_{\Theta}^T(x_{j+1})U_{\Theta}(x_{j+1}) - U_{\Theta}^T(x_{j+1})U_{\Theta}(X_j)[U_{\Theta}^T(X_j)U_{\Theta}(X_j)]^{-}U_{\Theta}^T(X_j)U_{\Theta}(x_{j+1})} \\ &= \frac{\{U_{\Theta}^T(x_{j+1})[I - U_{\Theta}(X_j)[U_{\Theta}^T(X_j)U_{\Theta}(X_j)]^{-}U_{\Theta}^T(X_j)]U_{\Theta}(x)\}^2}{U_{\Theta}^T(x_{j+1})[I - U_{\Theta}(X_j)[U_{\Theta}^T(X_j)U_{\Theta}(X_j)]^{-}U_{\Theta}^T(X_j)]U_{\Theta}(x_{j+1})}, \end{aligned}$$

where $[U_{\Theta}^T(X_j)U_{\Theta}(X_j)]^{-}$ is the generalized inverse of $[U_{\Theta}^T(X_j)U_{\Theta}(X_j)]$.

Let $C_{\Theta, X_j}(t) = [I - U_{\Theta}(X_j)[U_{\Theta}^T(X_j)U_{\Theta}(X_j)]^{-1}U_{\Theta}^T(X_j)]U_{\Theta}(t)$. Then,

$$\begin{aligned} & C_{\Theta, X_j}^T(x_{j+1})C_{\Theta, X_j}(x) \\ &= U_{\Theta}^T(x_{j+1})[I - U_{\Theta}(X_j)[U_{\Theta}^T(X_j)U_{\Theta}(X_j)]^{-1}U_{\Theta}^T(X_j)]U_{\Theta}(x). \end{aligned}$$

Similarly,

$$C_{\Theta, X_j}^T(x_{j+1})C_{\Theta, X_j}(x_{j+1}) = U_{\Theta}^T(x_{j+1})[I - U_{\Theta}(X_j)[U_{\Theta}^T(X_j)U_{\Theta}(X_j)]^{-1}U_{\Theta}^T(X_j)]U_{\Theta}(x_{j+1}).$$

Therefore,

$$R(x_{n+1}) \approx \frac{(C_{\Theta, X_j}^T(x_{j+1})C_{\Theta, X_j}(x))^2}{C_{\Theta, X_j}^T(x_{j+1})C_{\Theta, X_j}(x_{j+1})} = \|C_{\Theta, X_j}(x)\|_2^2 \cos^2(\vartheta),$$

where ϑ is the angle between $C_{\Theta, X_j}(x)$ and $C_{\Theta, X_j}(x_{j+1})$.

References

- Bawa, M., Condie, T., and Ganesan, P. (2005). Lsh forest: self-tuning indexes for similarity search. In *Proceedings of the 14th international conference on World Wide Web*, pages 651–660. ACM.
- Bellosta, C. J. G. (2015). *rPython: Package Allowing R to Call Python*. R package version 0.0-6.
- Bentley, J. L. (1975). Multidimensional binary search trees used for associative searching. *Communications of the ACM*, 18(9):509–517.
- Cangelosi, A. and Parisi, D. (2012). *Simulating the evolution of language*. Springer Science & Business Media.
- Datta, A., Banerjee, S., Finley, A. O., and Gelfand, A. E. (2015). Hierarchical nearest-neighbor Gaussian process models for large geostatistical datasets. *Journal of the American Statistical Association*, to appear. arXiv:1406.7343.
- Eckstein, W. (2013). *Computer simulation of ion-solid interactions*, volume 10. Springer Science & Business Media.
- Fang, K.-T., Li, R., and Sudjianto, A. (2005). *Design and modeling for computer experiments*. CRC Press.
- Furrer, R., Genton, M. G., and Nychka, D. (2006). Covariance tapering for interpolation of large spatial datasets. *Journal of Computational and Graphical Statistics*, 15(3).
- Gramacy, R. B. and Apley, D. W. (2015). Local gaussian process approximation for large computer experiments. *Journal of Computational and Graphical Statistics*, 24(2):561–578.
- Gramacy, R. B. and Haaland, B. (2015). Speeding up neighborhood search in local gaussian process prediction. *Technometrics*, (just-accepted).
- Gramacy, R. B., Niemi, J., and Weiss, R. M. (2014). Massively parallel approximate gaussian process regression. *SIAM/ASA Journal on Uncertainty Quantification*, 2(1):564–584.
- Haaland, B., Qian, P. Z., et al. (2011). Accurate emulators for large-scale computer experiments. *The Annals of Statistics*, 39(6):2974–3002.
- Harville, D. A. (1997). *Matrix algebra from a statistician’s perspective*, volume 157. Springer.

- Indyk, P. and Motwani, R. (1998). Approximate nearest neighbors: towards removing the curse of dimensionality. In *Proceedings of the thirtieth annual ACM symposium on Theory of computing*, pages 604–613. ACM.
- Jain, P., Kulis, B., and Grauman, K. (2008). Fast image search for learned metrics. In *Computer Vision and Pattern Recognition, 2008. CVPR 2008. IEEE Conference on*, pages 1–8. IEEE.
- Jones, E., Oliphant, T., Peterson, P., et al. (2001). SciPy: Open source scientific tools for Python.
- Liu, Y. and Hung, Y. (2015). Latin hypercube design-based block bootstrap for computer experiment modeling. Technical report, Rutgers.
- Nychka, D., Bandyopadhyay, S., Hammerling, D., Lindgren, F., and Sain, S. (2014). A multi-resolution gaussian process model for the analysis of large spatial data sets. *Journal of Computational and Graphical Statistics*, (just-accepted):00–00.
- Paciorek, C. J., Lipshitz, B., Zhuo, W., Kaufman, C. G., Thomas, R. C., et al. (2013). Parallelizing gaussian process calculations in r. *arXiv preprint arXiv:1305.4886*.
- Pedregosa, F., Varoquaux, G., Gramfort, A., Michel, V., Thirion, B., Grisel, O., Blondel, M., Prettenhofer, P., Weiss, R., Dubourg, V., Vanderplas, J., Passos, A., Cournapeau, D., Brucher, M., Perrot, M., and Duchesnay, E. (2011). Scikit-learn: Machine learning in Python. *Journal of Machine Learning Research*, 12:2825–2830.
- Plumlee, M. (2014). Fast prediction of deterministic functions using sparse grid experimental designs. *Journal of the American Statistical Association*, 109(508):1581–1591.
- R Core Team (2015). *R: A Language and Environment for Statistical Computing*. R Foundation for Statistical Computing, Vienna, Austria.
- Sacks, J., Welch, W. J., Mitchell, T. J., and Wynn, H. P. (1989). Design and analysis of computer experiments. *Statistical science*, pages 409–423.
- Santner, T. J., Williams, B. J., and Notz, W. I. (2013). *The design and analysis of computer experiments*. Springer Science & Business Media.
- Wendland, H. (2004). *Scattered data approximation*, volume 17. Cambridge university press.
- Williams, C. and Seeger, M. (2001). Using the nyström method to speed up kernel machines. In *Proceedings of the 14th Annual Conference on Neural Information Processing Systems*, number EPFL-CONF-161322, pages 682–688.
- Zhu, H., Williams, C. K., Rohwer, R., and Morciniec, M. (1997). Gaussian regression and optimal finite dimensional linear models.